# Semi-active Vibration Control Based on Switched Piezoelectric Transducers

Hongli Ji, Jinhao Qiu and Pinqi Xia
*Nanjing University of Aeronautics and Astronautics*
*China*

## 1. Introduction

Vibration in modern structures like airplanes, satellites or cars can cause malfunctions, fatigue damages or radiate unwanted and loud noise (Simpson & Schweiger, 1998; Wu et al., 2000; Hopkins et al., 2000; Kim et al., 1999; Zhang et al., 2001; Hagood et al., 1990). Since conventional passive damping materials have reached their limits to damp vibration because it is not very effective at low frequencies and requires more space and weight, new control designs with novel actuator systems have been proposed. These so called smart materials can control and suppress vibration in an efficient and intelligent way without causing much additional weight or cost. The vast majority of research in smart damping materials has concentrated on the control of structures made from composite materials with embedded or bonded piezoelectric transducers because of their excellent mechanical-electrical coupling characteristics. A piezoelectric material responds to mechanical force by generating an electric charge or voltage. This phenomenon is called the direct piezoelectric effect. On the other hand, when an electric field is applied to the material mechanical stress or strain is induced; this phenomenon is called the converse piezoelectric effect. The direct effect is used for sensing and the converse effect for actuation. The methods of vibration control using piezoelectric transducers can be mainly divided into three categories: passive, active, and semi-active. Passive control systems, which use the *R-L* shunting (Hagood & Crawley, 1991; Hollkamp, 1994), are simplest among the three categories, but their control performance is sensitive to the variations of the system parameters. Moreover, the passive control systems usually need large inductance in low frequency domain, which is difficult to realize. Active control systems require high-performance digital signal processors and bulky power amplifiers to drive actuators, which are not suitable for many practical applications.

In order to overcome these disadvantages, several semi-active approaches have been proposed. Wang et al. (1996) studied a semi-active *R-L* shunting approach, in which an adaptive inductor tuning, a negative resistance and a coupling enhancement set-up lead to a system with damping ability. Davis et al. (1997, 1998) developed a tunable electrically shunted piezoceramic vibration absorber, in which a passive capacitive shunt circuit is used to electrically change the piezoceramic effective stiffness and then to tune the device response frequency. Clark, W. W. (1999) proposed a state-switched method, in which piezoelements are periodically held in the open-circuit state, then switched and held in the short-circuit state, synchronously with the structure motion.

Another type of semi-active control, which has been receiving much attention in recent years, is called pulse switching technique (Richard et al., 1999, 2000; Onoda et al., 2003; Makihara et al., 2005). It consists in a fast inversion of voltage on the piezoelement using a few basics electronics, which is synchronized with the mechanical vibration. In the methods proposed by Richard et al. (1999) the voltage on the piezoelectric element is switched at the strain extrema or displacement extrama of vibration. These methods are called Synchronized Switch Damping (SSD) techniques. On the other hand, in the method proposed by Onoda and Makihara the switch is controlled by an active control theory and it is called active control theory based switching technique here (Onoda et al., 2003; Makihara et al., 2005).

In this chapter, the semi-active control methods based on state-switched piezoelectric transducers and pulse-switched piezoelectric transducers are introduced (Qiu et al., 2009). The semi-active approaches have several advantages compared to the passive and active methods: it is not sensitive to the variation of the parameters of system, and its implementation is quite simple, requiring only few small electronic components. It may use inductors, but much smaller than the ones needed by passive technique. So the control system is more compact compared with active control and passive control.

## 2. Modeling of a structural system with piezoelectric transducers

### 2.1 Equivalent SDOF model

A mechanical model based on a spring-mass system having only one degree of freedom gives a good description of vibrating behavior of a structure near a resonance (Badel et al., 2006; Ji et al., 2009a). The following differential equation is established assuming that the global structure including piezoelectric elements is linearly elastic:

$$M\ddot{u} + C\dot{u} + K_E u = \sum F_i \tag{1}$$

where $M$ represents the equivalent rigid mass, $C$ is the inherent structural damping coefficient, $K_E$ is the equivalent stiffness of the structural system, including the host structure and piezoelectric elements in short-circuit, $u$ is the rigid mass displacement and $\sum F_i$ represents the sum of other forces applied to the equivalent rigid mass, comprising forces applied by piezoelectric elements. The equivalent stiffness $K_E$ can be expressed as

$$K_E = K_s + K^{sc} \tag{2}$$

where $K_s$ is the stiffness of the host structure and the $K^{sc}$ is the stiffness of the piezoelectric transducer in short circuit. Piezoelectric elements bonded on the considered structure ensure the electromechanical coupling, which is described by

$$F_p = -\alpha V \tag{3}$$

$$I = \alpha \dot{u} - C_0 \dot{V} \tag{4}$$

where $F_p$ is the electrically dependent part of the force applied by piezoelectric elements on the structure, $C_0$ is the blocked capacitance of piezoelectric elements, $\alpha$ is the force factor, and $I$ is the outgoing current from piezoelectric elements. $M$, $C_0$, $\alpha$ and $K_E$ can be deduced from piezoelectric elements and structure characteristics and geometry.

Finally, $\sum F_i$ applied to the rigid equivalent mass comprises $F_p$ and an external excitation force $F$. Thus, the differential equation governing the mass motion can be written as

$$M\ddot{u} + C\dot{u} + K_E u = F - \alpha V \tag{5}$$

The following energy equation is obtained by multiplying both sides of the above equation by the velocity and integrating it over the time variable.

$$\int_0^T F\dot{u}dt = \frac{1}{2}M\dot{u}^2\Big|_0^T + \frac{1}{2}K_E u^2\Big|_0^T + \int_0^T C\dot{u}^2 dt + \int_0^T \alpha V\dot{u}dt \tag{6}$$

This equation exhibits that the provided energy is divided into kinetic energy, potential elastic energy, mechanical losses, and transferred energy. In the steady-state vibration, the terms of potential energy and kinetic energy in Eq. (6) disappear. The provided energy is balanced by the energy dissipated on the mechanical damper and the transferred energy, which corresponds to the part of mechanical energy which is converted into electrical energy. Maximizing this energy amounts to minimize the mechanical energy in the structure (kinetic + elastic).

If the frequency of excitation equals the resonance frequency of the system, the velocity of the mass, $\dot{u}$, can be considered to be in phase with the excitation force $F(t)$. In that case, the provided energy and the energy dissipated on mechanical damper are

$$\int_0^T F\dot{u}dt = F_M u_M \pi \quad \text{and} \quad \int_0^T C\dot{u}^2 dt = C\omega_0 u_M^2 \pi \tag{7}$$

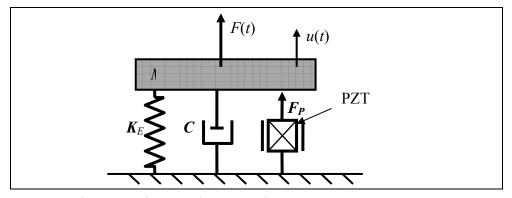where $F_M$ is the amplitude of the excitation force.



Fig. 1. A single SDOF with a piezoelectric transducer

## 2.2 A system with a shunt circuit

In passive control, the piezoelectric transducer in a structural system is connected to an electrical impedance (Hagood, 1991). In semi-active control, the piezoelectric transducer is usually connected to a switching shunt circuit, which is electrically nonlinear (Clark, 2000). When the piezoelectric transducer is connected to an electrical impedance $Z^{su}$, Eq. (4) becomes

$$\tilde{V} = \frac{s\alpha^2 Z^{su}}{sC_0 Z^{su} + 1}\tilde{u} \tag{8}$$

in the Laplace domain, where $\tilde{V}$ and $\tilde{u}$ are the Laplace transformation of $V$ and $u$, and $s$ is the Laplace variable. Substitution of Eq. (8) into the Laplace transformation of Eq. (5) gives the transfer function from excitation force $F$ to displacement response $u$ as follows

$$\tilde{u} / \tilde{F} = \frac{1}{Ms^2 + Cs + K_E + \dfrac{s\alpha^2 Z^{su}}{sC_0 Z^{su} + 1}} \tag{9}$$

where $\tilde{F}$ is the Laplace transformation of $F$. In passive control, optimal control performance is achieved by tuning the electrical impedance, $Z^{su}$, of the shunt circuit. However, the control performance of a passive control system deteriorates drastically when the $Z^{su}$ is detuned. Hence a passive control system is very sensitive to the variation of the system parameters and has low robustness.

Several semi-active approaches have been proposed to overcome the disadvantages of passive control systems. One is to adaptively tune the impedance, $Z^{su}$, of the shunt circuit. The second is to switch the shunt circuit between the states with different impedances. The third is to invert the voltage on the piezoelectric transducer by synchronically pulse-switching the shunt circuit.

### 2.3 Different states of piezoelectric transducer

(1) Short circuit condition

In the short circuit condition, the impedance of the shunt circuit connected to the piezoelectric transducer is zero ($Z^{su}=0$) and no electric power is dissipated, either. In the frequency domain, Equations (8) and (9) can be expressed as

$$\tilde{V} = 0 \, , \quad \frac{\tilde{u}}{\tilde{F}} = \frac{1}{\left( K_E - M\omega^2 + jC\omega \right)} \tag{10}$$

It is assumed that at the resonance frequency the force $F$ and the speed $\dot{u}$ are in phase (this is a good approximation for structures with low viscous losses). The resonance angular frequency and the amplitude of the displacement are given by

$$\omega_0^{sc} = \sqrt{\frac{K_E}{M}} \, , \quad u_M = \frac{F_M}{C\omega_0} \, . \tag{11}$$

where $F_M$ is this amplitude of the driving force. In the short circuit condition, the provided energy is balanced by the mechanical loss.

(2) Open circuit condition

In the open circuit condition of the piezoelectric elements, the impedance of the shunt circuit is infinity ($Z^{su}=\infty$) and no electric power is dissipated, either. In the frequency domain, Equations (8) and (9) can be expressed as

$$\tilde{V} = \frac{\alpha}{C_0} \tilde{u} \, , \quad \frac{\tilde{u}}{\tilde{F}} = \frac{1}{\left( K_E + \dfrac{\alpha^2}{C_0} - M\omega^2 + jC\omega \right)} \tag{12}$$

For the same reason as for the short circuit case, the resonance angular frequency and the amplitude of the displacement are given by.

$$\omega_0^{oc} = \sqrt{\frac{K_E + \frac{\alpha^2}{C_0}}{M}} \, , \ u_M = \frac{F_M}{C\omega_0^{oc}} \, . \tag{13}$$

Obviously, the stiffness of the piezoelectric transducer in the open circuit condition is

$$K^{oc} = K^{sc} + \frac{\alpha^2}{C_0} \, . \tag{14}$$

The piezoelectric transducer exhibits higher stiffness in the open circuit condition and the resonance frequency of the system in open circuit condition is higher than that in the short circuit condition. The voltage on the piezoelectric transducer and the displacement and velocity of the mass are illustrated in Fig.2. In this state, the net converted energy from mechanical to electrical in a cycle of vibration is zero, that is, the last term in Eq. (6) is zero.
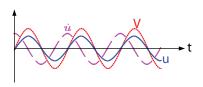


Fig. 2. Voltage, displacement and velocity in the open circuit condition

Obviously, the difference between the resonance frequency in the short circuit condition and that in the open circuit condition is due to the electro-mechanical coupling of the piezoelectric transducer in the structure. To quantitatively characterize its electro-mechanical property, the following parameter, $k_{struct}$, is defined as the electro-mechanical coupling factor of the structure:

$$k_{struct} = \frac{\left(\omega_0^{oc}\right)^2 - \left(\omega_0^{sc}\right)^2}{\left(\omega_0^{sc}\right)^2} \, . \tag{15}$$

The resonance frequencies, $\omega_0^{oc}$ and $\omega_0^{sc}$, of the structure with the piezoelectric transducer under open and short circuit conditions, respectively, can easily be measured experimentally. Hence the electro-mechanical coupling factor of the structure can easily be estimated from experimentally results. After $k_{struct}$ is obtained, the force factor, $\alpha$, can easily be calculated from the following equation:

$$\alpha = k_{struct}\omega_0^{sc}\sqrt{C_0} \, . \tag{16}$$

(3) Resistive shunt condition

When the piezoelectric transducer is shunted by a resistor $R$, that is, $Z^{su}=R$, Equations (8) and (9) can be expressed as

$$\tilde{V} = \frac{j\rho\omega/\omega_n}{j\rho\omega/\omega_n + 1} \cdot \frac{\alpha^2}{C_0}\tilde{u} \ ,$$

$$\frac{\tilde{u}}{\tilde{F}} = \frac{1}{\left( K_E - M\omega^2 + jC\omega + \dfrac{j\rho\omega/\omega_n}{j\rho\omega/\omega_n + 1} \cdot \dfrac{\alpha^2}{C_0} \right)} \tag{17}$$

in the frequency domain, where $\omega_n$ is an arbitrary angular frequency for non-dimensionalization and $\rho = \omega_n C_0 R$ is the non-dimensional resistance. The condition $R=0$ corresponds to short circuit and $R=\infty$ corresponds to the open circuit condition.

Resistive shunt has been widely used in passive damping based on piezoelectric transducers. An optimal resistance can be obtained by minimizing the magnitude of the transfer function from $\tilde{F}$ to $\tilde{u}$ at the resonance frequency of the system. In the next section the control performance of the state-switched approach is compared with that of the resistive shunt.

## 3. The state-switched approach

The state-switched method has been successfully used in semi-passive vibration absorbers (Cunefare, 2002) and semi-passive vibration damping using piezoelectric actuator (Clark 1999, 2000; Corr & Clark 2001). Only the state-switched approach using piezoelectric actuators is discussed in this section. In the state-switched approach using piezoelectric actuators, a piezoelectric actuator is switched between the high- and low-stiffness states using a simple switching logic to achieve vibration suppression, essentially storing energy in the high-stiffness state and dissipating a part of the that energy in the switching process between the low-stiffness state and high-stiffness state. As shown in the Section 2.3, the piezoelectric transducer has different stiffness for different electrical boundary conditions (short circuit or open circuit). Different from the pulse-switched approach introduced in the next section, this approach keeps the piezoelectric element in each of the high- and low-stiffness states for one quarter-cycle increments.

The energy loss in a state-switched system can be explained by a mass-spring system as shown in Fig. 3 (Corr & Clark, 2001). The stiffness of the spring, $K^*$, in the system can be switched between two states: $K^{HI}$ and $K^{LO}$, with $K^{HI} > K^{LO}$. As the mass move away from its equilibrium position, the stiffness of the spring is set to $K^{HI}$. When the mass reaches its maximum displacement the potential energy is at a maximum:

$$U_{\max} = K^{HI}u_M^2 \tag{18}$$

At this point, the stiffness of the variable spring is changed from $K^{HI}$ to $K^{LO}$. Now the potential energy of the system is less than before. The difference in energy is

$$\Delta U = \frac{1}{2}\left(K^{HI} - K^{LO}\right)u_M^2 \ . \tag{19}$$

Hence, there is $\Delta U$ less potential energy to be converted back to kinetic energy, that is, the system has lost some of its total energy. The variable spring is left in the $K^{LO}$ state until the mass goes back to its original equilibrium point. At this time, the variable spring is again changed to $K^{HI}$ state and the cycle repeats itself.
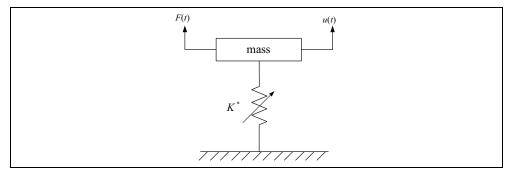
Fig. 3. A SDOF system with a variable spring

In theory, one could continuously vary the resistance in the circuit in real time to obtain a completely variable semi-active system. An alternative is to simply switch between states of the system. The two most straightforward scenarios are shown in Fig. 4(b) and 4(c), where switching occurs between the open and short circuit states (OC-SC), and between the open and resistive shunt states (OC-RS). (Note that switching between the short circuit and resistive shunt states will not be explored because neither of these states exhibits high-stiffness.) State-switching of the actuator is based on the following logic: Given the single degree-of-freedom system shown in Fig. 4, when the system is moving away from equilibrium, or

$$u\dot{u} > 0 \qquad (20)$$

the circuit is switched to the high-stiffness state (open circuit), and when the system is moving toward equilibrium,

$$u\dot{u} < 0 \qquad (21)$$

then the system is switched to the low-stiffness and/or dissipative state (short or resistive circuit). So during a full cycle of motion, switching occurs four times, once after each quarter cycle. At equilibrium the system is switched to a high stiffness, then at peak motion it is switched back to low stiffness and it returns to equilibrium to complete the half-cycle. At equilibrium again the system is switched to high stiffness, and the switching process repeats over the next half-cycle. This has the effect of suppressing deflection away from equilibrium, and then at the end of the deflection quarter-cycle, dissipating some of the stored energy so that it is not given back to the system in the form of kinetic energy.
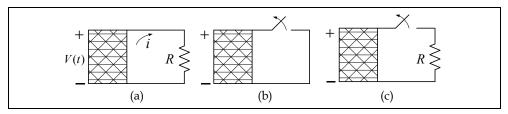


Fig. 4. Schematic of three piezoelectric configurations used in this study: (a) Passive resistive shunt; (b) State-switched: Open-circuit to short circuit; (c) State-switched: Open-circuit to resistive circuit

Now the SDOF system in Fig. 1 is considered. The mass is under excitation of a harmonic force $F(t)$ with an angular frequency of $\omega$ and its response is assumed to be a harmonic vibration of the same frequency. The piezoelectric transducer is switched between open circuit and short circuit using the switching strategy in Eqs. (20) and (21). The energy dissipated in a full cycle of vibration due to the switching actions is

$$
\begin{aligned}
E_{cycle}^{dis} &= \int_0^{T/4} K^{oc} u \dot{u} dt + \int_{T/4}^{T/2} K^{sc} u \dot{u} dt + \int_{T/2}^{3T/4} K^{oc} u \dot{u} dt + \int_{3T/4}^{T} K^{sc} u \dot{u} dt \\
&= (K^{oc} - K^{sc}) u_M^2 \\
&= \frac{\alpha^2}{C_0} u_M^2
\end{aligned}
\tag{22}
$$

In the open-circuit case, deflection stores energy by way of the mechanical stiffness and by the capacitance of the device, which also appears as a mechanical stiffness. When the system is then switched to the short circuit state, the charge stored across the capacitor is shunted to ground, effectively dissipating that portion of the energy, and the effective stiffness is decreased. Since the provided energy is balanced by the mechanical loss and the energy dissipated by the switched shunted circuit, the following equation holds when the system is excited at the resonance frequency:

$$
F_M u_M \pi = C \omega_0 u_M^2 \pi + \frac{\alpha^2}{C_0} u_M^2 .
\tag{23}
$$

The displacement amplitude of vibration is

$$
u_M = \frac{F_M}{C \omega_0 + \dfrac{\alpha^2}{\pi C_0}} .
\tag{24}
$$

To quantitatively evaluate the damping effect of a control method, a performance index $A$ is defined as follows

$$
A = 20 \log \left( \frac{\text{vibration amplitude with control}}{\text{vibration amplitude without control}} \right) .
\tag{25}
$$

The performance index of the state-switched control for a single-frequency vibration is given by

$$
A_{\text{State-swithing}} = 20 \log \left( \frac{C \omega_0}{C \omega_0 + \dfrac{\alpha^2}{\pi C_0}} \right) .
\tag{26}
$$

If on the other hand, the circuit is switched to the resistive shunt, then the electrical charge is dissipated through the resistor, and the effective stiffness is also decreased (an added benefit is that additional damping is obtained while the resistor is in the circuit during the next quarter cycle, so in some cases the OC-RS system can perform better than the OC-SC system.)

The damped impulse response of the OC-SC system can be compared to that of the other two systems of interest, that is, the RS system and the OC-RS system [Clark 2000]. The resistor used in both the RS circuit and that in the OC-RS circuit are chosen to be optimal. The results are shown in Fig. 5. Note that for the impulse response, it is better to use a resistor in the circuit during state-switching. It is also shown that slightly better damping can be achieved with the passive resistive shunt circuit. The effective damping ratios were calculated for each case by logarithmic decrement and are shown in Table 1.

| System | Effective Damping Ratio |
|--------|------------------------|
| Passive Resistive Shunt | 0.22 |
| State-Switched OC-SC | 0.12 |
| State-Switched OC-RS | 0.19 |

Table 1. Effective damping ratios for passive and state-switched systems

Even though the passive resistive shunt system provides slightly better performance than the state-switched systems for the optimized cases, it is interesting to note that the results change significantly when the resistors are no longer optimized. Simulations were performed on the impulse response of the same three systems when the mass and actuator material compliance are dramatically changed but the resistance values are held at their previous optimal values. The results showed that the state-switched systems are less sensitive to the change, seeing very little change in performance, with the OC-RS case still providing slightly better performance (note that the OC-SC case can be thought of as a lower limit on damping performance), but the passive resistive shunt case is much worse than before.
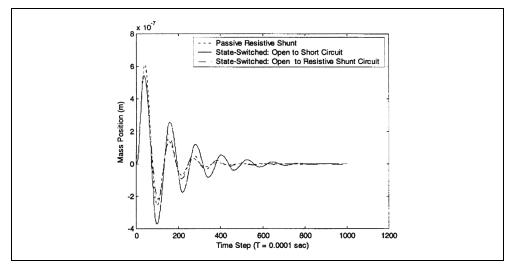


Fig. 5. Impulse response of passive resistive shunt, the OC-RS state switched, and OC-RS state-switched systems using optimal resistance
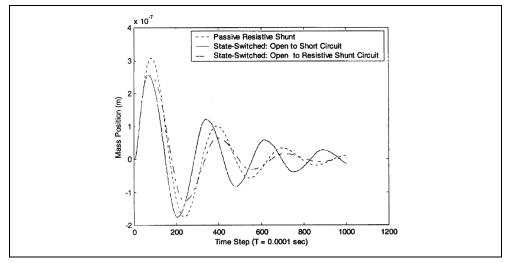
Fig. 6. Impulse response of passive resistive shunt, the OC-RS state switched, and OC-RS state-switched systems with non-optimal resistance

## 4. The pulse-switch methods

### 4.1 The Synchronized Switch Damping technique

The synchronized switch damping (SSD) method, also called pulse-switched method, consists in a nonlinear processing of the voltage on a piezoelectric actuator. It is implemented with a simple electronic switch synchronously driven with the structural motion. This switch, which is used to cancel or inverse the voltage on the piezoelectric element, allows to briefly connect a simple electrical network (short circuit, inductor, voltage sources depending on the SSD version) to the piezoelectric element. Due to this process, a voltage magnification is obtained and a phase shift appears between the strain in piezoelectric patch and the resulting voltage. The force generated by the resulting voltage is always opposite to the velocity of the structure, thus creating energy dissipation. The dissipated energy corresponds to the part of the mechanical energy which is converted into electric energy. Maximizing this energy is equivalent to minimizing the mechanical energy in the structure.

(1) The synchronized switch damping on short circuit

Several SSD techniques have been reported. The simplest is called SSDS, as shown in Figure 7(a), which stands for Synchronized Switch Damping on Short circuit (Richard et al., 1999, 2000). The SSDS technique consists of a simple switching device in parallel with the piezoelectric patch without other electric devices. The switch is kept open for most of the time in a period of vibration. It is closed when the voltage reaches a maximum (corresponding to a maximum of the strain in the piezoelectric patch) to dissipate all the electric energy in a short time (much shorter than the period of vibration) and then opened again. The voltage on the piezoelectric transducer is shown in Fig. 7(b). The maximum voltage on the piezoelectric transducer is
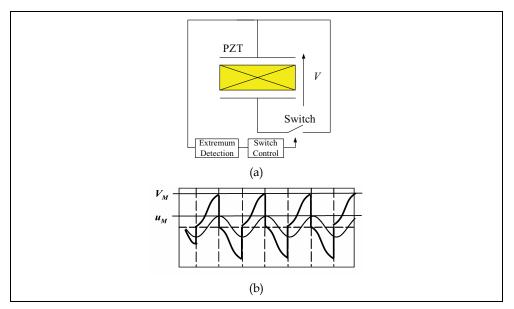
Fig. 7. The principle of SSDS technique

$$V_{Max} = \frac{2\alpha}{C_0} u_M \tag{27}$$

which is twice as large as that in the open circuit condition.

The maximum electric energy stored in the piezoelectric transducer can easily be calculated from the voltage in Eq. (27). This energy is dissipated when the voltage is discharged to zero at the maximum displacement point. In each cycle of mechanical vibration, the piezoelectric transducer is discharged twice. Hence, in the SSDS technique, the transferred energy $E_t$ in a period of single-frequency vibration is given by

$$E_t = \frac{4\alpha^2}{C_0} u_M^2 \tag{28}$$

The performance index of the SSDS damping for a single-frequency vibration is given by

$$A_{SSDS} = 20\log(\frac{C\omega_0}{C\omega_0 + \frac{4\alpha^2}{C_0\pi}}) \tag{29}$$

The above expressions exhibit that more energy is dissipated by the SSDS than by the state-switched shunt circuit in a single cycle of mechanical vibration and SSDS yields better control performance.

(2) The synchronized switch damping on inductor

To further increase the dissipated energy, the SSDI technique (synchronized switch damping on inductor) as shown in Fig. 8a has been developed by Richard et al. (2000),

Guyomar et al. (2001) and Petit et al. (2004). In the SSDI approach, an inductor is connected in series with the switch. Because the piezoelectric patch and the inductor constitute a *L-C* resonance circuit, fast inversion of the voltage on the piezoelectric patch is achieved by appropriately controlling the closing time and duration of the switch. The switch is closed at the displacement extremes, and the duration of the closed state is half the period of the *L-C* circuit. This leads to an artificial increase of the dissipated energy. The period of the *L-C* circuit is chosen to be much smaller than that of the mechanical vibration. The following relation holds between the voltage before inversion, $V_M$, and that after inversion, $V_m$,

$$V_m = \gamma V_M \,, \tag{30}$$

where $\gamma \in [0,1]$ is the voltage inversion coefficient. The inversion coefficient γ is a function of the quality factor of the shunt circuit. The larger the quality factor is, the larger the voltage inversion coefficient is. A typical value of $\gamma$ is between 0.6 to 0.9.



(a)  Schematic of the system
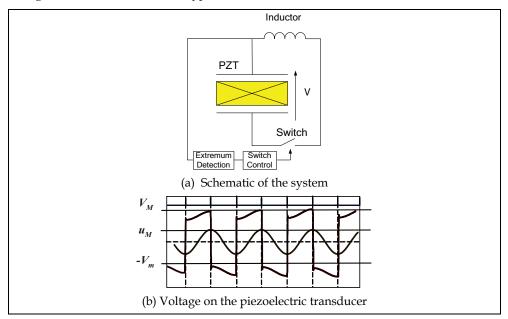
(b) Voltage on the piezoelectric transducer

Fig. 8. The principle of SSDI technique

As shown in Fig. 8(b), in the steady-state vibration the voltage on piezoelectric transducer increases from $V_m$ to $V_M$ between two switching points due to mechanical strain. Hence their difference is $V_{Max}$ given by Eq. (27). From these relationships, the absolute value of the average voltage between two switching points is

$$\frac{1}{2}(V_m + V_M) = \frac{1+\gamma}{1-\gamma}\frac{\alpha}{C_0}u_M \tag{31}$$

It indicates that the average voltage on the piezoelectric transducer has been amplified by a factor of $(1+\gamma)/(1-\gamma)$. The dissipated energy $E_t$ during a period of single-frequency vibration is given by

$$E_t = \frac{4\alpha^2}{C_0} \frac{1+\gamma}{1-\gamma} u_M^2 \tag{32}$$

Compared with Eq. (28) the transferred energy has also been magnified by a factor of $(1+\gamma)/(1-\gamma)$ (Badel et al., 2005). If the voltage inversion coefficient is 0.9, its value is 9.5. Hence, much better control performance can be achieved with SSDI. The theoretical damping value of the SSDI technique for a single-frequency vibration is

$$A_{SSDI} = 20\log(\frac{C\omega_0}{C\omega_0 + \frac{4\alpha^2}{\pi C_0} \frac{1+\gamma}{1-\gamma}}) . \tag{33}$$

## 4.2 The active control theory based switching law

Onoda and Makihara proposed a new switching law based on active control method (Onoda et al., 2003; Makihara et al. 2007c). As an example, the LQR (linear quadratic regulator) control law was used in their studies. The state equation of the plant to be controlled is assumed to be

$$\dot{\mathbf{z}} = \mathbf{Az} + \mathbf{Df} + \mathbf{BQ} \tag{34}$$

where $z$ is the state variable, $A$, $B$ and $C$ are state matrices, $f$ is the external disturbance, and $Q$ is the control input, which is the charges on the piezoelectric elements. A linear quadratic regulator is designed to minimized the performance index

$$J = \int (\mathbf{z}^T \mathbf{W}_1 \mathbf{z} + \mathbf{Q}^T \mathbf{W}_2 \mathbf{Q}) dt \tag{35}$$

where $W_1$ and $W_2$ are weight matrices. The control input can be expressed in the following form:

$$\mathbf{Q}_T = \mathbf{Fz} . \tag{36}$$

The regulator $F$ is given by

$$\mathbf{F} = \mathbf{W}_2^{-1} \mathbf{B}^T \mathbf{P} \tag{37}$$

where $P$ is a positive definite solution of

$$\mathbf{PBW}_2^{-1} \mathbf{B}^T \mathbf{P} - \mathbf{A}^T \mathbf{P} - \mathbf{PA} - \mathbf{W}_1 = 0 . \tag{38}$$

Usually the value of $z$ is difficult to measure and they estimated by an observer. When the estimated value of z is used, the active control input is obtained from

$$\mathbf{Q}_T = \mathbf{F}\hat{\mathbf{z}} . \tag{39}$$

where $\hat{\mathbf{z}}$ is the estimated value of $z$. Once the value of $Q_T$ is obtained, the switch in the shunt circuit for the ith piezoelectric actuator is controlled based on $Q_{Ti}$, which is the $i$th component in the $Q_T$, according to the switch control law discussed below.

It should be noted that in a semi-active control system, damping effect is achieved by switching shunt circuit, not by applying the control input $Q_T$ as in active control. In order to

obtain damping effect, a possible strategy to control the switch is to turn the switch on and off so that the charge $Q_i$ on the $i$th piezoelectric element traces $Q_{Ti}$ as closely as possible. However, in many cases, a large gain results in quick vibration damping. Therefore, the switch is controlled such a way that $\mathbf{Q}$ becomes as large, that is, positive, as possible when $\mathbf{Q}_T$ is positive, and as small, that is, negative, as possible when $\mathbf{Q}_T$ is negative. The study by Onoda et al. (1997) has shown that this strategy is more effective than tracing $\mathbf{Q}_T$, although the difference between their performances is small.

Based on the above discussion, the following control law can be obtained for switched $R$ shunt of a piezoelectric element: Turn on the switch when

$$Q_T V < 0 \, , \tag{40}$$

and turn off the switch when

$$Q_T V > 0 \, , \tag{41}$$

where $V$ is the voltage on the piezoelectric patch.

The switch control law for a piezoelectric element with a switched $L$-$R$ shunt can be expressed in the following form: Turn on the switch when

$$Q_T V < 0 \, , \tag{42}$$

and turn it off when

$$Q_T \dot{Q} < 0 \, . \tag{43}$$

Note that any active control theory can be used to obtain $Q_T$ of a piezoelectric though LQR control method has been used as an example above.

## 5. The SSDV approach

### 5.1 The classical SSDV technique

In order to further increase the damping effect, a method called SSDV (SSDV stands for synchronized switch damping on voltage) as shown in Fig. 9 was proposed by Lefeuvre et al. (2006), Makihara et al. (2005), Faiz et al. (2006), and Badel et al., (2006). In the case of the SSDV, a voltage source $V_{cc}$ is connected to the shunting branch, in series with the inductor, which can magnify the inverted voltage and hence improve the control performance. The absolute value of average voltage on piezoelectric transducer between two switching actions is (Badel, , et al., 2006)

$$V = (\frac{\alpha}{C_0} u_M + V_{cc}) \frac{1+\gamma}{1-\gamma} \, . \tag{44}$$

The dissipated energy during one period of vibration is a function of $u_M$ and $V_{cc}$ as follows:

$$E_t = (\frac{4\alpha^2}{C_0} u_M^2 + 4\alpha u_M V_{cc}) \frac{1+\gamma}{1-\gamma} \, . \tag{45}$$

The theoretical value of the SSDV damping is then given by

$$A_{SSDV} = 20\log\left(\frac{C\omega_0}{C\omega_0 + \dfrac{4\alpha^2}{C_0\pi}\dfrac{1+\gamma}{1-\gamma}} \times \left(1 - \frac{4}{\pi}\frac{1+\gamma}{1-\gamma}\frac{\alpha V_{cc}}{F_M}\right)\right), \tag{46}$$

where $F_M$ is the amplitude of excitation force $F_e$. The SSDV technique can achieve better vibration control performance than SSDI, but a stability problem arises due to the fact that the voltage source is kept constant. Equation (46) shows that under a given excitation force, the value of voltage source $V_{cc}$ that theoretically totally cancels the vibration can be found. This particular value is

$$V_{cc\,max} = \frac{\pi}{4\alpha}\frac{1-\gamma}{1+\gamma}F_M. \tag{47}$$

This is also the maximum voltage that can be applied in this excitation condition. Applying a voltage higher than $V_{cc\text{max}}$ leads to instability (experimental results actually show that stability problems occur before reaching this critical value).
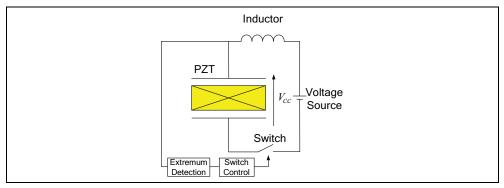


Fig. 9. The principle of SSDV technique

## 5.2 Adaptive SSDV techniques

Equation (47) shows that $V_{cc\text{max}}$ is proportional to the amplitude of the excitation. Hence if the voltage is adjusted according to the amplitude of the excitation, the stability problem can be solved. Accordingly the enhanced and adaptive SSDV techniques, in which the voltage is adjusted according to the amplitude of excitation, have been developed. In a real system, the amplitude of the excitation is usually unknown, but we can measure the vibration amplitude of the structure.

(1) Enhanced SSDV

In the enhanced SSDV proposed by Badel et al. (2006) the voltage source is proportional to the vibration amplitude as shown in following equation.

$$V_{cc} = -\beta\frac{\alpha}{C_0}u_M, \tag{48}$$

where $\beta$ is the mentioned voltage coefficient. In the Enhanced SSDV, the dissipated energy $E_t$ during a period can be expressed as

$$E_t = \frac{4\alpha^2}{C_0}(1+\beta)\frac{1+\gamma}{1-\gamma}u_M^2 \, . \tag{49}$$

Compared with the classical SSDV technique, the enhanced SSDV increases the transferred energy, which results in an increase in the vibration damping. The theoretical value of damping of the enhanced SSDV is given by

$$A_{SSDV_{enh}} = 20\log(\frac{C\omega_0}{C\omega_0 + \frac{4\alpha^2}{C_0\pi}(1+\beta)\frac{1+\gamma}{1-\gamma}}) \, . \tag{50}$$

Equation (50) shows that, for a given value of parameter $\beta$, the damping is not sensitive to the amplitude of the applied force. This is the critical point of the enhanced SSDV. But it must be noted that for large value of $\beta$, the above theoretical expressions are no longer valid because the displacement of high-order modes cannot be neglected any longer compared to the fundamental one. From the experimental results it has been found that the optimal value of the voltage coefficient $\beta$ depends on many factors such as the noise level of the measured signal, the property of the switch, et al. Hence, in order to achieve optimal control performance, the voltage coefficient should be adjusted adaptively according to the vibration amplitude and other experimental conditions.

(2) Derivative-based adaptive SSDV

An adaptive enhanced SSDV technique, in which the voltage coefficient is adjusted adaptively to achieve optimal control performance, has been proposed by Ji et al. (2009a). The basic principle of the adaptive SSDV technique is that the coefficient $\beta$ is adjusted based on the sensitivity of the vibration amplitude with respect to $\beta$: the more the vibration amplitude is sensitive to $\beta$, the more $\beta$ is increased. If the variation of amplitude is $\Delta u_{Mi}$ due to an increment of the voltage coefficient $\Delta\beta_i$, the sensitivity is defined as $\Delta u_{Mi}/\Delta\beta_i$. The increment of the voltage coefficient, $\Delta\beta_{i+1}$, in the next step is defined as

$$\Delta\beta_{i+1} = -\eta\frac{\Delta u_{Mi}}{\Delta\beta_i} \, , \tag{51}$$

where $\eta$ is the convergence rate factor. The larger the factor $\eta$ is, the faster the convergence rate is. But when $\eta$ is too large, the iteration process may become unstable. The physical meaning of the algorithm defined in Eq.(51) is similar to the Newton-Raphson method in numerical analysis.

Since $\Delta u_{Mi}/\Delta\beta_i$ is an approximation of the derivative of amplitude $u_M$ with respect to $\beta$, this approach is called derivative-based adaptive SSDV. In the real system, $\Delta\beta_i$ is not updated in each cycle of vibration because of the noise in the measured amplitude. Instead, $\Delta\beta_i$ is kept constant for $n$ cycles and the amplitudes $u_{Mk}$ (k=1,…,n) are recorded. A parabolic curve is then fitted from the points $u_{Mk}$ and the slope at the final point $u_{Mn}$ is defined as the sensitivity.

(3) LMS-based adaptive SSDV

In the derivative-based adaptive SSDV, the voltage coefficient $\beta$ is optimized to achieve good damping control performance. Actually, the final goal of optimizing voltage coefficient

$\beta$ is to obtain the optimal voltage. A novel adaptive SSDV method based on LMS algorithm to adjust the voltage source directly or voltage coefficient was proposed by Ji et al. (2009b).

In the LMS-based adaptive SSDV, a FIR filter is used to optimize the voltage $V_{cc}$ or the voltage coefficient $\beta$. Their values are defined at each switching point (each displacement extrema), not the discrete sampling time $n$. Hence the detected displacement amplitude $u_M$ (which is used as a sensor signal to control the switch action) (Ji et al., 2009b), instead of the displacement $u$ itself, is used as the error $e$ to the FIR filter. The output $y$ of the FIR filter is the voltage or the voltage coefficient $\beta$ at the switching times, instead of the voltage value at each discrete time, and the calculated voltage is held constant until the next switching time so that a rectangular wave is generated automatically by the switching circuit. Hence the LMS-based system is a sub-system which is not executed at each discrete time, but triggered and executed at each detected extrema. The diagram of a LMS-based adaptive SSDV control system is shown in Fig. 10. In the case of the optimization of $\beta$, the value of $\beta$ is calculated from

$$\beta(n') = \mathbf{h}(n') * \mathbf{u}_m(n'-1) = h(1)u_m(n'-1) + h(2)u_m(n'-2) + \cdots + h(m)u_m(n'-m) \tag{52}$$

where $\mathbf{h}$ is an FIR filter, $n'$ is the discrete time defined at the detected extrema. This means that $n'-1$ represent the discrete time at the previous detected extremum. After $\beta$ is calculate from Eq. (52), the voltage $V_{cc}$ is obtained from Eq. (46). This method can be considered as an extension of the enhanced SSDV. In the case of the direct optimization of the voltage $V_{cc}$, the following equation is used:

$$V_{cc}(n') = \mathbf{h}(n') * \mathbf{u}_m(n'-1) = h(1)u_m(n'-1) + h(2)u_m(n'-2) + \cdots + h(m)u_m(n'-m). \tag{53}$$

Since the voltage is directly optimized by this method, it can be considered as an improvement to the classical SSDV, where the voltage source is fixed. The same symbol $\mathbf{h}$ is used in Eqs. (52) and (53), but they have different values.

It should be noted that although the standard LMS algorithm has been used in this study, its implementation is not standard. The LMS-based is masked and executed only at the discrete time defined at the detected extrema, $n'$, at which the FIR filter is updated and the control input is calculated. Due to the non-standard implementation, the other LMS-based control laws, such as the Filtered-X algorithm, is difficult to apply in this system.
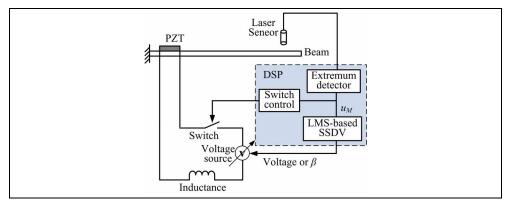


Fig. 10. The diagram of a LMS-based adaptive SSDV control system

# Thank You for previewing this eBook

You can read the full version of this eBook in different formats:

> ➢ HTML (Free /Available to everyone)

> ➢ PDF / TXT (Available to V.I.P. members. Free Standard members can access up to 5 PDF/TXT eBooks per month each month)

> ➢ Epub & Mobipocket (Exclusive to V.I.P. members)

To download this full book, simply select the format you desire below